Hole injection barriers at polymer anode/small molecule interfaces

A. J. Mäkinen,[a] I. G. Hill, R. Shashidhar, N. Nikolov, and Z. H. Kafafi
U.S. Naval Research Laboratory, Washington, DC 20375

(Received 15 March 2001; accepted for publication 25 May 2001)

A photoemission study of the interface between spin-cast films of a conducting polymer blend consisting of poly(3,4-ethylenedioxythiophene) (PEDOT), poly(4-styrenesulfonate) (PSS) and glycerol as an additive, and vacuum-evaporated hole transport layers (HTL) of 4,4′-bis(carbazol-9-yl)biphenyl, N,N′-diphenyl-N,N′-bis(1-naphthyl)-1-1′biphenyl-4,4′-diamine and N,N′-diphenyl-N,N′-bis(3-methylphenyl)-1,1′- biphenyl-4,4′-diamine reveals a hole injection barrier between 0.5 and 0.9 eV at the glycerol-modified PEDOT-PSS/HTL interface. The measured energy barriers imply a reasonable charge injection, which is very encouraging for further development of the novel anode structures based on a conducting polymer/small molecule interface to be utilized in electro-optic applications such as organic light-emitting devices. © *2001 American Institute of Physics.* [DOI: 10.1063/1.1386400]

Despite the recent success in the commercialization of flat panel display technology utilizing organic light-emitting diodes (OLEDs), the research in the field continues to be challenged by both fundamental scientific and technological issues, such as device efficiency and reliability, color tunability, and the cost of fabrication. An additional set of challenges applies to OLED-based flexible displays. These include identifying flexible and transparent substrate materials with low gas permeability for oxygen and water, researching anode and cathode materials compatible with these substrates and suitable for large area deposition. Attempts to find a possible alternative to the common transparent anode material, indium tin oxide (ITO), used in molecular and polymeric OLEDs have focused on conducting polymers.

Highly doped conjugated polymers have many attractive properties such as good electrical conductivity and work functions equal to or higher than that of ITO. However, in achieving a high enough conductivity, the transparency of the polymer film is often compromised. Earlier reports comprised the use of a conducting polymer in combination with ITO as an anode structure, such as polyaniline (PANI)-coated ITO electrodes in polymeric devices.[1–3] In these studies, it was found that the introduction of the bilayer anode structure reduced the operating voltage and increased the electroluminescence quantum efficiency, which was attributed to a lower hole injection barrier between the anode and the hole-transporting emissive layer.[1,2] The ITO/PANI electrodes were also found to have smoother surfaces than bare ITO resulting in fewer shorts and improved device reliability. More recently, films of polymer blends of poly(3,4-ethylenedioxythiophene) (PEDOT) and poly(4-styrenesulfonate) (PSS) have been used as spacer layers between the ITO electrode and the hole-transporting luminescent polymer.[4–6] The ITO/PEDOT-PSS-based devices were found to perform equally well as the ITO/PANI-based devices, and interestingly, the device lifetime increased after eliminating the ITO underlayer all together from the OLED structures.[5]

In this letter, we report a photoemission study of the interface formation between spin-cast films of a variation of the PEDOT-PSS system and vacuum-evaporated hole transport (HT) materials, 4,4′-bis(carbazol-9-yl)biphenyl (CBP), N,N′-diphenyl-N,N′-bis(1-naphthyl)-1-1′biphenyl-4,4′-diamine (α-NPD) and N,N′-diphenyl-N,N′-bis(3-methylphenyl)-1,1′-biphenyl-4,4′-diamine (TPD) (see Fig. 1 for the chemical structures). Employing recently developed fabrication methods in preparing the PEDOT-PSS films resulted in polymer films with low sheet resistance without compromising the transparency of the film. PEDOT-PSS films typically have a sheet resistance of 500 Ω/□ with 75% transmission for visible light.[6] The PEDOT-PSS films reported in this letter have sheet resistances and transparencies in the range of 350-500 Ω/□ and 80%–85%, respectively. Most notably, the film transparency was found to be *independent* of the sheet resistance of the polymer films contrary to previously reported PEDOT-PSS films.[7] Here the increased conductivity is achieved through nonionic doping described below without increasing the optical density of the polymer films, which will be discussed in detail in a future publication. Our ultraviolet photoemission spectroscopy (UPS) results indicate that the hole injection barrier is between 0.5 and 0.9 eV at the interface of the PEDOT-PSS film and the studied hole transport layers (HTLs). In the best case, the obtained energy barrier is roughly a factor of 2 smaller than the barriers measured for the PEDOT-PSS/hole-

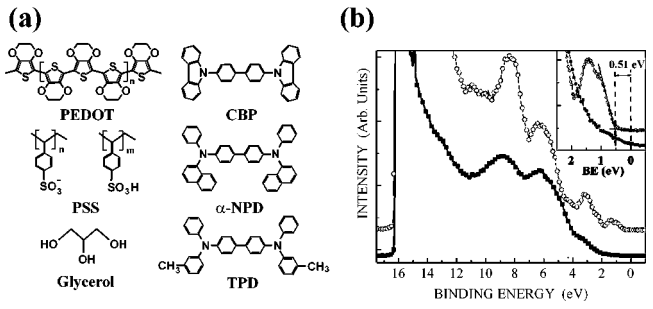

FIG. 1. (a) Chemical structures of the investigated materials. (b) HeI spectra of a bare G-PEDOT film (solid squares) and covered with a 25-Å-thick α-NPD film (open circles). The inset shows the low binding energy (BE) part of the spectra.

[a]Electronic mail: ajm@ccs.nrl.navy.mil

transporting luminescent polymer [poly(bis-(2-dimethyl-octylsilyl)-1,4-phenylvinylene or poly(9,9-dioctylfluorene] interfaces.[8,9] This finding is highly relevant for device design since the overall quantum and luminous power efficiencies of an OLED device are greatly influenced by the injection efficiency of electrons and holes at the respective electrode/organic interfaces.

The PEDOT-PSS films were prepared from an aqueous dispersion (10 ml) containing a 0.8 molar ratio of PEDOT and PSS, purchased from Bayer (Baytron P V4071), to which 0.6 g of glycerol and 1 ml of methanol were added. In the following, we will abbreviate the glycerol-modified PEDOT-PSS system as G-PEDOT. After spin coating the G-PEDOT films onto bare or ITO-coated glass and Si substrates, they were baked at 125 °C for 5 min, rinsed with methanol, dried and inserted into UHV. The thickness of the G-PEDOT films was between 400 and 500 nm. The UPS measurements were carried out in a two-chamber UHV system (base pressure 10^{-10} Torr) with a preparation and an analysis chamber separated by a gate valve. The HTLs were vacuum-evaporated onto the G-PEDOT films. Photoemission spectra of the films were recorded for HeI ($h\nu = 21.22$ eV) and HeII ($h\nu = 40.82$ eV) radiation using a hemispherical energy analyzer for electron detection. The resolution of the analyzer was set to 50 meV. The sample was biased at -3.0 V to compensate for the contact potential between the sample and the analyzer.

The film deposition was done layer by layer, and the UPS spectra were recorded after each deposition. The HeI spectra for a G-PEDOT film on a bare glass substrate and for a 25-Å-thick α-NPD layer on the G-PEDOT film are shown in Fig. 1 where the binding energy is referenced to the Fermi level (E_F) of the analyzer. The HeI spectrum of the G-PEDOT film reveals molecular orbital structures at binding energies above 2 eV, but between 2 eV and E_F the spectrum appears featureless. Although we measure a finite number of counts at E_F (compared with the counts above 0 eV) we observe no clear emission cutoff. Therefore, we could not determine the E_F directly from the UPS spectra of the G-PEDOT films. Instead, we obtained the position of the E_F from a separately recorded HeI spectrum of a sputter-cleaned Ag foil. Using the E_F and the vacuum level onset energy determined from the HeI spectra of the G-PEDOT films we calculated the work function of the films. Due to the metallic nature of the highly doped G-PEDOT films, the E_F of the film is expected to align with the E_F of the analyzer. This method gives a work function value of 4.9–5.0 eV for the investigated G-PEDOT films. The HeI spectra were also recorded for G-PEDOT films spincast onto ITO-glass and Si substrates. The vacuum level onset energy and consequently the position of E_F were found to be the same as for the films coated onto bare glass substrates.

The low binding energy orbital structure of the α-NPD overlayer has much more distinct features than the bare G-PEDOT. The two highest occupied molecular orbitals (HOMO and HOMO-1) form a double feature observed between 0.5 and 2.0 eV, which was additionally verified from the HeII spectra of the α-NPD overlayer. The HOMO position was determined from the edge of the emission cutoff by linear extrapolation as shown in the inset of Fig. 1, and it

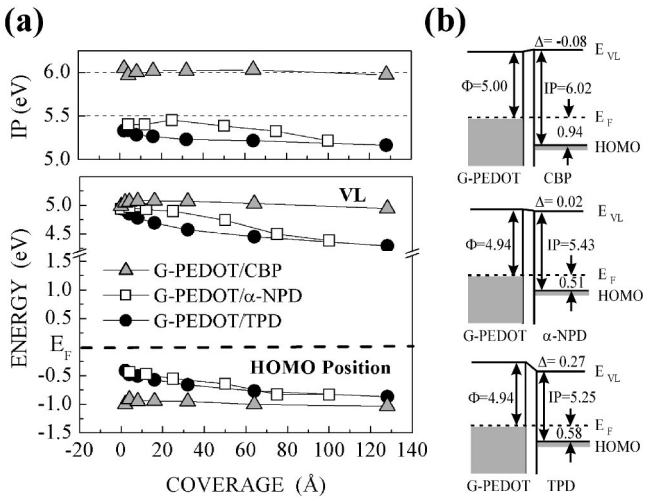

FIG. 2. (a) The ionization potential (IP), vacuum level (VL) and HOMO positions of CBP, α-NPD and TPD, deposited on G-PEDOT, as a function of their film thickness. (b) Energy level diagram of the G-PEDOT/CBP, G-PEDOT/α-NPD, and G-PEDOT/TPD interfaces. All energies are expressed in electron volts (eV).

was found to be approximately 0.5 eV below the E_F. In a photoemission experiment, the HOMO level marks the highest occupied energy level of a cation with a net positive charge of one, and hence the E_F-HOMO separation is equal to the energy barrier for hole injection from the conductor into the organic. We also observe that the vacuum levels of the α-NPD overlayer and the G-PEDOT film are practically aligned as indicated by the overlapping intensity onset values of the spectra in Fig. 1. Consequently, it is essentially the difference between the work function of the conducting polymer film and the ionization potential of the hole transport layer that determines the hole injection barrier between the two films. In other words, Schottky–Mott rule seems to apply to charge injection at this interface.[10]

A summary of the results based on the above analysis on the spectra of CBP, α-NPD, and TPD overlayers is presented in Fig. 2 where the evolution of the energy level positions is plotted as a function of the respective overlayer thickness. The vacuum levels of the α-NPD layer and the G-PEDOT film align through coverage of 0–50 Å after which there is a shift of 0.20 eV. The α-NPD HOMO position follows the behavior of the vacuum level so that after remaining constant for the first 50 Å coverage, it drops by the same amount as the vacuum level. The identical movement of both the vacuum level and the HOMO position after 50 Å coverage indicates a rigid shift of the entire HeI spectrum. For this reason, the ionization potential (IP) remains constant (5.41 eV) as seen in Fig. 2. This is most likely caused by slight charging of the thicker overlayers. Since α-NPD is primarily a hole transport material[11] its electron mobility is expected to be very small, which is likely to result in incomplete balancing of the emitted charge during the photoemission experiment.

The vacuum level and the HOMO position of the CBP overlayers behave very similarly. In this case, the overall shift of the vacuum level stays constant up to a 32 Å thickness after which both the HOMO and the vacuum level shift rigidly towards higher binding energy. The IP is unaffected by the spectrum shift and is 6.02 eV for the CBP overlayers.

In contrast to the constant vacuum level of CBP and α-NPD overlayers, the vacuum level of the TPD layer is first seen to undergo an abrupt shift of 0.27 eV during the first part of deposition (4–16 Å), after which the rate of shift decreases. The vacuum level shift during the initial stages of the overlayer growth implies a formation of a small interface dipole within the first monolayer.[12] This is in agreement with the observed overlayer thicknesses where the substrate is expected to be fully covered within the first 10–15 Å. As in the case of CBP and α-NPD overlayers, the simultaneous and equal shift of the HOMO and vacuum level positions of the TPD layers at higher coverages (>32 Å) is attributed to the charging of the overlayers. Again, the IP does not change significantly between 32 and 64 Å, and is found to be 5.25 eV.

When estimating the energy barriers for charge injection at interfaces it is critical to be able to distinguish between the real level shifts due to the structure of the interface and the artificial ones due to, e.g., charging. Therefore, we have determined the position of the energy levels used in the diagram in Fig. 2 from spectra taken on overlayers less than 32 Å thick. Based on the measured energy level positions, we have prepared an energy level diagram for the G-PEDOT/CBP, the G-PEDOT/α-NPD and the G-PEDOT/TPD interfaces shown in Fig. 2. The vacuum level and HOMO positions have been determined from the ''flat band'' region shown in Fig. 2 as explained above. From the device engineering point of view the most critical parameter shown in the energy level diagrams is the E_F–HOMO separation, i.e., the barrier for hole injection. This energy is 0.94, 0.51, and 0.58 eV for the G-PEDOT/CBP, G-PEDOT/α-NPD, and G-PEDOT/TPD interfaces, respectively. The measured barrier heights compare extremely well with the reported 0.8 eV barrier at the ITO/α-NPD and with the 0.5 eV barrier at the ITO/TPD interfaces.[12,13] These results are therefore very encouraging for further development of polymer/small molecule interfaces. The fabrication and characterization of OLEDs based on these anode structures are in progress, and will be reported in a future publication.

The E_F–HOMO separation at the anode interface shown in Fig. 2 is intimately related to the magnitude of the ionization potential (IP) of the HTL, the vacuum level shift (Δ) and the work function (Φ) of the anode material. The vacuum levels at the G-PEDOT/CBP and the G-PEDOT/α-NPD interfaces are practically aligned ($\Delta_{\mathrm{CBP}}=-0.08$ eV, $\Delta_{\alpha-\mathrm{NPD}}=0.02$ eV) given the 0.1 eV resolution of the photoemission method, whereas there is a vacuum level shift of 0.27 eV at the G-PEDOT/TPD interface. The difference in the vacuum level shifts between α-NPD and TPD is relatively close to the difference between the IPs of α-NPD and TPD, i.e., $\Delta_{\mathrm{TPD}}-\Delta_{\alpha-\mathrm{NPD}}=0.25$ eV and $\mathrm{IP}_{\alpha-\mathrm{NPD}}-\mathrm{IP}_{\mathrm{TPD}}=0.18$ eV. The relationship between the ionization potential of an overlayer and the vacuum level shift at a conductor/organic interface has previously been pointed out by Ishii and Seki,[14] and it is attributed to the limited movement of E_F in the gap of the organic semiconductor. In other words, a sufficiently high density of gap states of the organic layer (due to impurity levels, defect states, or metal-induced gap states) can pin E_F in a certain position limiting its movement upon interface formation. Interestingly, the HOMO–E_F separation at the two polymer/small molecule interfaces is almost the same, and given the similar optical band gap energies of α-NPD and TPD, ~ 3.1 eV,[15] we can view the position of E_F within each band gap the same. Since the substrate work function and the band gaps of the HTLs are the same at the investigated interfaces, the change in the vacuum level shift (Δ) is then largely determined by the change in the IP of the HT layer, i.e., $\Delta=\mathrm{IP}-\Phi-(E_F-\mathrm{HOMO})$.

It is, however, important to note that the movement of E_F is unrestricted deeper in the TPD gap. This has been shown for Al/TPD ($E_F-\mathrm{HOMO}=1.7$ eV) and for Au/TPD ($E_F-\mathrm{HOMO}=1.3$ eV) interfaces in recent photoemission experiments.[14] Similarly, the CBP overlayer has a significantly higher IP (6.02 eV) than α-NPD (5.43 eV) or TPD (5.25 eV), and therefore E_F is located closer to the middle of the gap (~ 3.1 eV, as estimated from optical absorption[15]). Since there is no considerable vacuum level shift, this implies that E_F can move unrestricted in this part of the CBP gap.

In conclusion, we have studied the interface formation between films of G-PEDOT and CBP, α-NPD and TPD and found the hole injection barriers of 0.94, 0.51, and 0.58 eV at the respective interfaces. These energy barriers are comparable to those measured for ITO/α-NPD and ITO/TPD interfaces. This result is very encouraging for further development of the novel anode structures based on a conducting polymer/small molecule interface.

This research was funded by ONR. One of the authors (A.J.M.) acknowledges the NRC for administering the postdoctoral program at NRL.

[1] Y. Yang and A. J. Heeger, Appl. Phys. Lett. **64**, 1245 (1994).
[2] A. J. Heeger, I. D. Parker, and Y. Yang, Synth. Met. **67**, 23 (1994).
[3] S. Karg, J. C. Scott, J. R. Salem, and M. Angelopoulos, Synth. Met. **80**, 111 (1996).
[4] J. C. Scott, S. A. Carter, S. Karg, and M. Angelopoulos, Synth. Met. **85**, 1197 (1997).
[5] S. A. Carter, M. Angelopoulos, S. Karg, B. J. Brock, and J. C. Scott, Appl. Phys. Lett. **70**, 2067 (1997).
[6] Y. Cao, G. Yu, C. Zhang, R. Menon, and A. J. Heeger, Synth. Met. **87**, 171 (1997).
[7] R. Shashidhar, Y. Miao, and N. Nikolov, Patent Application, Navy Case No. 82,573 (Sep. 13, 2000).
[8] Th. Kugler, W. R. Salaneck, H. Rost, and A. B. Holmes, Chem. Phys. Lett. **310**, 391 (1999).
[9] G. Greczynski, Th. Kugler, and W. R. Salaneck, J. Appl. Phys. **88**, 7187 (2000).
[10] G. Greczynski, M. Fahlman, and W. R. Salaneck, Chem. Phys. Lett. **321**, 379 (2000).
[11] M. Stolka, J. F. Yanus, and D. M. Pai, J. Phys. Chem. **88**, 4707 (1984).
[12] H. Ishii, K. Sugiyama, E. Ito, and K. Seki, Adv. Mater. **11**, 605 (1999).
[13] Q.-T. Le, E. W. Forsythe, F. Neuesch, L. J. Rothberg, L. Yan, and Y. Gao, Thin Solid Films **363**, 42 (2000).
[14] H. Ishii and K. Seki, IEEE Trans. Electron Devices **44**, 1295 (1997).
[15] I. G. Hill, D. Milliron, J. Schwartz, and A. Kahn, Appl. Surf. Sci. **166**, 354 (2000); A. J. Mäkinen, S. Schoemann, Y. Gao, M. G. Mason, A. A. Muenter, and A. R. Melnyk, Proc. SPIE **3940**, 65 (2000).